

Contemporary vertical velocity of the central Basin and Range and uplift of the southern Sierra Nevada

Noah P. Fay,¹ Richard A. Bennett,¹ and Sigrún Hreinsdóttir¹

Received 1 July 2008; revised 18 September 2008; accepted 24 September 2008; published 28 October 2008.

[1] We estimate the present-day vertical velocity field in the central Basin and Range and Sierra Nevada mountains and consider causative processes. We analyzed data from 16 continuously operating Global Positioning System stations finding that relative vertical velocity precision (WRMS scatter) is ~ 0.25 mm/yr. These data demonstrate that the southern Sierra Nevada is experiencing uplift of ~ 0.5 mm/yr relative to a local reference frame in southern Nevada, and ~ 1 mm/yr relative to stations in the northern Mojave Desert. As a possible source of these motions, we explored post-seismic viscoelastic relaxation following the 1872 Owens Valley and 1952 Kern County earthquakes with models of laterally homogeneous lower crust and upper mantle viscosity. Post-seismic deformation from these two earthquakes cannot entirely explain the data set. Lateral variations in viscosity or contributions from other regional earthquakes may also be important. **Citation:** Fay, N. P., R. A. Bennett, and S. Hreinsdóttir (2008), Contemporary vertical velocity of the central Basin and Range and uplift of the southern Sierra Nevada, *Geophys. Res. Lett.*, 35, L20309, doi:10.1029/2008GL034949.

1. Introduction

[2] The formation and uplift of mountain ranges is a fundamental component of continental deformation associated with plate tectonics. The vertical history of the Sierra Nevada (SN) Mountains, the remnant of Cretaceous arc magmatism [e.g., Ducea, 2001] and western margin of the extensional Basin and Range province, is debated. A diverse body of evidence suggests that the $\sim 3\text{--}5$ Ma removal of the gravitationally unstable eclogitic root of the granitic batholith [e.g., Zandt *et al.*, 2004] prompted a significant uplift event [Jones *et al.*, 2004]. However, geochemical and thermochronological tracers of paleoelevation and relief on and around the SN suggest that it has seen little increase in average elevation during the late Cenozoic [e.g., House *et al.*, 1998; Mulch *et al.*, 2006].

[3] The present-day vertical deformation field may provide useful constraint on lithospheric rheology and possibly a datum from which to work backwards in time to constrain the vertical history of the range. To do so, long-lived transient vertical motions, such as caused by post-seismic stress relaxation [e.g., Gourmelen and Amelung, 2005], need to be quantified. In this paper we present vertical velocity estimates for the southern SN and surroundings through analysis of more than 8 years of continuous Global

Positioning System (CGPS) data (Figure 1) and estimate the vertical velocities caused by postseismic viscoelastic relaxation following two recent large earthquakes.

2. GPS Data and Analysis

[4] The CGPS stations used in this study (Figure 1) were chosen based on their similar data quality, duration of operation and the fact that they form a linear array approximately perpendicular to the strike of the SN batholith and major faults accommodating relative SN-Basin and Range horizontal motion (Figure 1). The stations began operating in 1999 and 2000 as a part of the SCIGN [Hudnut *et al.*, 2001] and BARGEN [Wernicke *et al.*, 2000] CGPS networks. GPS phase data were processed following Bennett and Hreinsdóttir [2007] and Bennett *et al.* [2007]. We used the GAMIT/GLOBK software [King and Bock, 2002; Herring, 2002] version 10.3 incorporating IGS absolute phase center models and the stable North American reference frame (SNARF) of Blewitt *et al.* [2005]. The horizontal velocities at the CGPS stations in our study area (Figure 1; see also Table S1¹) clearly demonstrate the dominant regional horizontal tectonics, i.e., right-lateral shear accommodating the NW motion of the SN relative to the continental interior [e.g., Wernicke and Snow, 1998].

[5] Vertical positions and velocities derived from CGPS are inherently less precise than the horizontal components, owing to a number of imperfectly understood hydrologic and atmospheric processes that load the Earth's surface and displace its center of mass [Blewitt *et al.*, 2001]. However, these issues do not necessarily prevent precise determination of relative vertical motions over relatively short baselines (e.g., 500 km) [Bennett and Hreinsdóttir, 2007; Bennett *et al.*, 2007]. We consider here only relative vertical velocities that allow us to safely ignore long-wavelength vertical signals that effectively cancel in a locally-defined vertical reference frame.

[6] One such example of common-mode "noise" that does not significantly bias relative vertical velocity estimates is shown in Figure 2. Figure 2a shows the vertical position timeseries of station BEPK that typifies the timeseries of all of the stations in our study area. There is a clear vertical signal with an apparent period of ~ 5.5 yrs (apparent because we do not have a complete cycle). We estimate the magnitude and phase of this signal with a weighted least squares fit to the timeseries including terms accounting for coseismic and radome vertical offsets, a constant velocity, annual and semi-annual periodic signals, and a periodic signal with period of 5.5 years (determined iteratively). The average amplitude of this 5.5 year signal is $\sim 2.7 \pm 0.5$ mm.

¹Department of Geosciences, University of Arizona, Tucson, Arizona, USA.

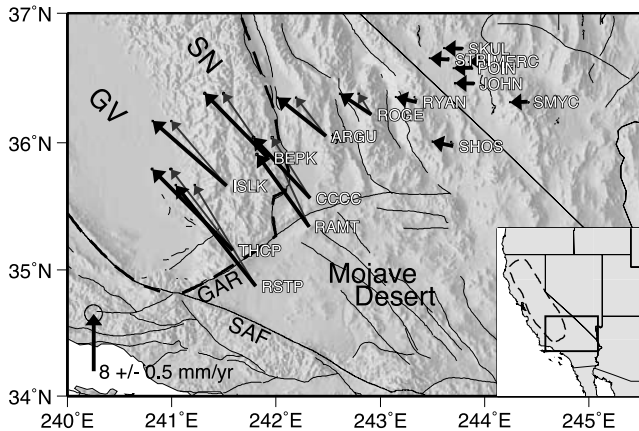


Figure 1. Shaded relief map of study area showing major geographic features (SN, Sierra Nevada; GV, Great Valley), fault traces (thin black lines, SAF, San Andreas fault, GAR, Garlock fault), and CGPS stations. The thick black vectors show horizontal velocity relative to stable North America, and thin grey vectors show horizontal velocity relative to the average velocity of the 5 Yucca Mountain reference sites (SKUL, STRI, MERC, POIN, JOHN). Error ellipses represent 95% confidence. Dashed line (also in inset map) shows the outline of the SN block.

[7] The stations in our study area are generally in phase with respect to the 5.5 year signal. This can be seen in Figure 2b where we show the average residuals (observed minus linear, annual and semianual signals) for the days common to the five Yucca Mountain sites defining our local reference frame (JOHN, MERC, POIN, SKUL and STRI). Subtracting these mean residuals from the other stations' timeseries results in a statistically significant (>99% confidence) reduction in the weighted root mean square of their residuals indicating the 5.5 year period signal is indeed common to all sites and thereby does not affect the relative vertical velocities. The slopes of the adjusted timeseries represent the velocities relative to the average of the 5 reference sites. These velocities (Figure 3; see also Table S1) are not significantly different from the relative velocities determined directly from the GLOBK velocity solution. We do not know the cause of the 5.5 year signal although it is unlikely to be a tectonic process.

[8] Stations within the SN (THCP, ISLK, BEPK) show a consistent positive vertical velocity of ~ 0.5 mm/yr. Stations to the south and southeast of the SN (RSTP, RAMT, CCC) show a consistent negative vertical velocity of 0.4–0.75 mm/yr. Uncertainties on these relative rates derived from either the formal uncertainty estimates in GLOBK or the common-mode least squares analysis are between 0.1 and 0.2 mm/yr and have been scaled such that the normalized RMS of the 5 reference stations is unity. The WRMS of the reference stations near the tectonically stable Yucca Mountain is ~ 0.25 mm/yr and provides another measure of velocity precision [Davis et al., 2003]. The least squares normalized misfit (reduced χ^2 statistic) is less than 0.5 for all the stations indicating the velocity uncertainties are perhaps conservative and effectively, albeit informally, compensate for possible temporal correlations in the times-

eries, which are low for these stations [e.g., Langbein, 2008].

3. Uplift Processes and Modeling

[9] Point measurements of uplift determined by CPGS provide estimates of rock uplift, not necessarily surface uplift [England and Molnar, 1990]. However, because (1) nearby stations within and adjacent to the SN are consistent in rate with their neighbors, and (2) the vertical velocities within the SN outpace modern fluvial and regional erosion rates by an order of magnitude or more [Stock et al., 2005], the vertical velocities we observe likely represent true surface uplift.

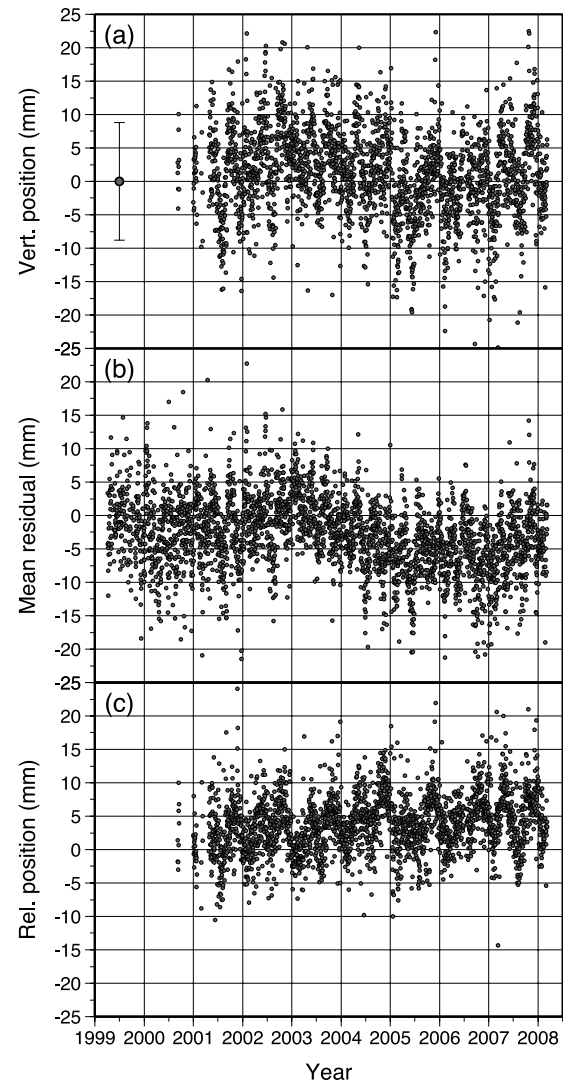


Figure 2. (a) Vertical position timeseries for station BEPK (North America reference frame). Error bars are omitted for clarity. The large dot at 1999.5 yrs., 0 mm, shows the mean uncertainty (one standard error). Coseismic offsets caused by regional earthquakes (e.g., 1999 Hector Mine) have been removed from the timeseries. (b) Mean residuals (position minus best-fit seasonal terms) for the days common to the 5 Yucca Mountain reference stations. (c) BEPK's vertical position timeseries relative to the reference stations' mean, i.e., Figure 2a minus Figure 2b.

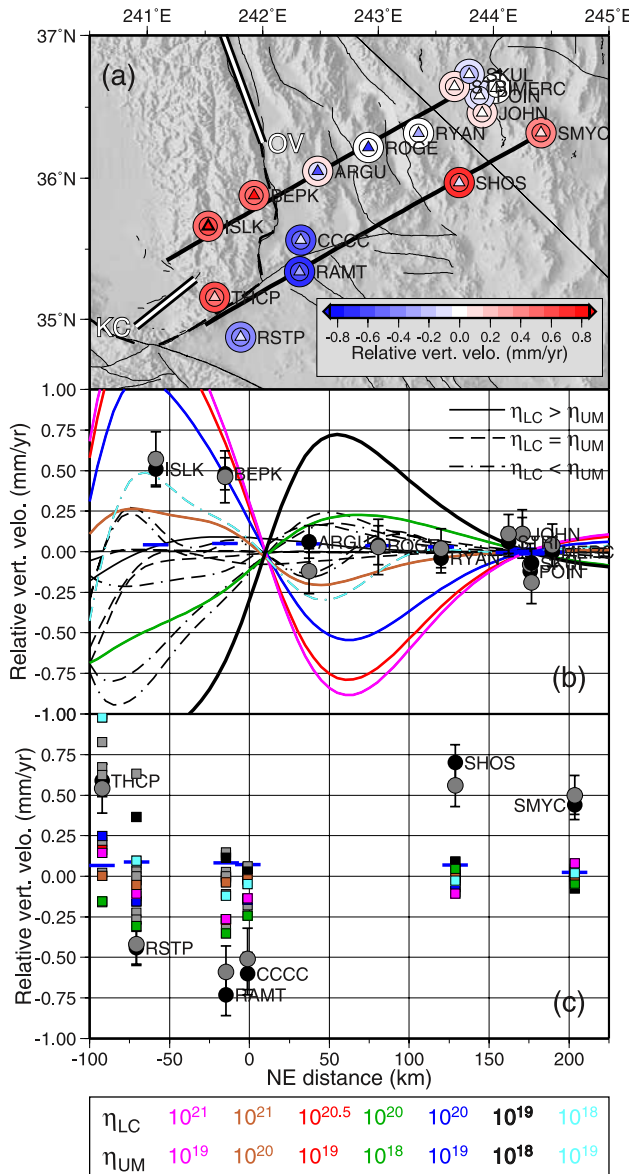


Figure 3. (a) Relative vertical velocity determined directly from the GLOBK velocity solution (large solid circles) and with the common-mode least squares timeseries analysis (small solid circles). Velocities are relative to the average of SKUL, STRI, MERC, POIN, and JOHN. Solid triangles show the predicted relative vertical velocity utilizing the viscosity structure of *Hammond et al.* [2008]. Double black lines show the surface trace of modeled earthquakes. NE–SW black lines show the profiles used in Figures 3b and 3c. (b) Observed and predicted relative vertical velocity as function of distance NE of the OV earthquake. Black dots show relative vertical velocity derived from the GLOBK velocity solution and grey dots from the least squares analysis. Error bars give one standard error uncertainties. Curves show the predicted vertical velocity along the northern NE–SW profile in Figure 3a. A few models are highlighted in color and discussed in the text; see legend for corresponding viscosity (Pa·s) distribution. Blue horizontal bars show the predicted long-wavelength glacial isostatic rebound velocity [*Blewitt et al.*, 2005]. (c) Same as in Figure 3b for stations along the southern NE–SW profile. Predicted velocity shown for each station is shown with the squares.

[10] There are a number of possible processes to produce uplift of the Earth's surface. These can be divided into (1) short-term or transient, and (2) long-term or time-invariant processes. Short-term processes occur over relatively short time intervals (e.g., 10–10,000 yrs.), and transient processes produce vertical velocity that is not steady in rate or sign. These processes may produce little net regional vertical displacement. The most likely processes relevant to the study area include post-seismic relaxation [e.g., *Freed et al.*, 2007], interseismic loading of active faults in the southernmost SN block [e.g., *Stein and Thatcher*, 1981], and glacial loading and unloading [Granger and Stock, 2004].

[11] Long-term and time-invariant processes occur on time scales on the order of 1 million years and may produce significant regional vertical displacement. These processes include the isostatic and flexural response to surface loads [e.g., *Small and Anderson*, 1995; *Pelletier*, 2004]; uplift [e.g., *Le Pourhiet et al.*, 2006] and flexure [*Saleeby and Foster*, 2004] related to delamination; the flexural and isostatic response to crustal extension [e.g., *Wernicke and Axen*, 1988]; and thermally driven uplift [*Saltus and Lachenbruch*, 1991].

[12] Given the magnitudes of uplift of the SN relative to southern Nevada (~0.5 mm/yr) or the northern Mojave province (~1 mm/yr), it is difficult to argue that these surface motions are steady in time and long lived; 1 mm/yr of uplift over 1 million years produces 1 km of relief and the present-day relief between the southernmost SN (Tehachapi mountains) and northern Mojave desert is only ~650 meters. Therefore either a significant fraction of the observed vertical motions result from deformation processes that are transient in space or time, or we must conceive of a time-invariant process that is nascent or has been active for only a short duration (≤ 1 Myr.). The negligible mean vertical velocity (<0.1 mm/yr relative to North America) and absence of a systematic pattern (e.g., uniform tilt) suggests the dominance of local processes.

[13] The key to determining which processes are responsible for the observed uplift and subsidence pattern is careful forward modeling of each to determine their spatial and temporal characteristics. We begin by considering the role of post-seismic viscoelastic relaxation following the 1872 M_w 7.5–7.7 Owens Valley (OV) and 1952 M_w 7.3 Kern County (KC) earthquakes (Figure 3a). The OV earthquake was primarily a right-lateral strike-slip event with an average of 6 m of horizontal and 1 m of normal offset [Beanland and Clark, 1994]. The KC was a left-lateral (~3.6 m offset) and thrust (~1.6–1.9 m offset) earthquake [Bawden, 2001].

[14] We calculate the vertical velocity at present caused by viscoelastic relaxation of the stresses induced by these earthquakes in a simplified gravitational earth model consisting of a layered viscoelastic halfspace using the method and code presented by *Wang et al.* [2006]. The rheology is linear Maxwell viscoelastic with a 15 km elastic crust overlying a 15 km viscoelastic lower crust overlying a semi-infinite viscoelastic upper mantle. The earthquakes extend to the base of the 15 km thick elastic layer. The elastic properties of the model domain are constant throughout (shear modulus of 30 GPa, Poisson's ratio of 0.25). The surface velocities caused by the KC and OV

earthquakes are linearly dependent on the magnitude of imposed slip because we use a linear rheology.

[15] We have calculated 16 models to systematically explore the range of viscosities, 10^{18} – 10^{21} Pa-s, that likely exist in the lower crust and upper mantle in this region [e.g., Thatcher and Pollitz, 2008]. In addition, we calculated one additional model utilizing the preferred viscosity distribution for this region of Hammond *et al.* [2008] (lower crust $10^{20.5}$ Pa-s, upper mantle 10^{19} Pa-s). The predicted relative vertical velocities for these models are shown in Figure 3. We show the time-averaged velocity over the period 2000–2008. All models with no viscosity contrast across the Moho (dashed curves) predict ~zero velocity for the northern profile (Figure 3b). Models with upper mantle viscosity greater than the lower crust (dash-dot-dash curves) all predict relatively small vertical velocities ($\leq\sim 0.25$ mm/yr) or significant subsidence in the SN. Models with lower crust viscosity greater than that in the upper mantle (solid curves) predict both uplift and subsidence of the SN depending on the viscosity structure. For example, the blue curve (lower crust 10^{21} Pas, upper mantle 10^{19} Pas) and black curve (lower crust 10^{19} Pas, upper mantle 10^{18} Pas) are similar in form but opposite in sign. This is because there is a reversal in sign of vertical velocity in the vicinity of the surface rupture and the time between the earthquake and the reversal depends on the viscosity structure; the former model has not experienced this reversal whereas the latter has.

4. Discussion and Conclusions

[16] The postseismic models most successful at predicting uplift of the southern SN, at least to the north of the Kern County event, are those with a lower crust viscosity higher than that of the upper mantle (blue, red, pink curves in Figure 3b) [Thatcher and Pollitz, 2008]. These models tend to correctly predict the vertical velocity of BEPK but overpredict ISLK by a factor of 2 or more. However, both lateral variations in viscosity (strong SN lithosphere) and non-Newtonian rheology will produce smaller vertical velocities in the SN long after (e.g., 100 yrs.) the OV earthquake. The large regional heat flow gradient [Erkan and Blackwell, 2008] suggests the SN lithosphere may be of significantly higher viscosity than the surroundings and therefore would see damped postseismic velocities throughout the earthquake cycle [Malservisi *et al.*, 2001]. Non-Newtonian rheology will also result in reduced velocities long after the event because stresses will be relaxed faster immediately after the earthquake. These effects will also decrease the magnitude of the subsidence predicted for the stations to the east of the SN (ARGU, ROGE, RYAN), in better agreement with the negligible velocities observed there.

[17] The model most successful at predicting the subsidence pattern in the Mojave (RSTP, RAMT, CCCC) also utilizes a relatively high viscosity lower crust (green curve in Figure 3b). However, it significantly underpredicts uplift throughout the southern SN. This demonstrates the general result that it is difficult to find a single viscosity structure that can explain all of the observations (the maximum variance reduction for all models is $\sim 30\%$). However, postseismic relaxation still remains likely to be necessary

because none of the other processes alone are capable of producing the spatial variability in the observations. Continental-scale post-glacial rebound is unlikely to be important here because it predicts essentially uniform and negligible rates (<0.1 mm/yr, see Figures 3b and 3c). Regional post-glacial unloading of the SN [Granger and Stock, 2004] may be invoked to explain the uplift of ILSK and BEPK, and interseismic elastic loading of the White Wolf fault may account for a portion of uplift observed at THCP, but neither are capable of producing the subsidence of RSTP, RAMT, CCCC, and uplift of SHOS and SMYC. It is possible that relaxation following large unknown events (e.g., prior to 1872) or more recent events, such as the 1992 Landers and 1999 Hector Mine earthquakes [e.g., Freed *et al.*, 2007], may contribute to the vertical motions in our study area. The analysis of numerous additional CGPS stations as they mature and further numerical modeling will allow an explicit test of this hypothesis and utilization of precise vertical GPS measurements to constrain tectonic processes.

[18] **Acknowledgments.** Thorough reviews by an anonymous reviewer and Roland Bürgmann led to important improvements in the manuscript. This research was supported by NSF grant EAR-0545519 and the Southern California Earthquake Center. SCEC is funded by NSF Cooperative Agreement EAR-0106924 and USGS Cooperative Agreement 02HQAG0008. The SCEC contribution number for this paper is 1223.

References

- Bawden, G. W. (2001), Source parameters for the 1952 Kern County earthquake, California: A joint inversion of leveling and triangulation observations, *J. Geophys. Res.*, **106**, 771–785.
- Beanland, S., and M. M. Clark (1994), The Owens Valley Fault Zone, eastern California, and surface faulting associated with the 1872 earthquake, *U.S. Geol. Surv. Bull.*, **1982**, 29 pp.
- Bennett, R., and S. Hreinsdóttir (2007), Constraints on relative vertical crustal motion for long baselines in the central Mediterranean region using continuous GPS, *Earth Planet. Sci. Lett.*, **257**, 419–434, doi:10.1016/j.epsl.2007.03.008.
- Bennett, R. A., S. Hreinsdóttir, M. S. Velasco, and N. P. Fay (2007), GPS constraints on vertical crustal motion in the northern Basin and Range, *Geophys. Res. Lett.*, **34**, L22319, doi:10.1029/2007GL031515.
- Blewitt, G., D. Lavallee, P. Clarke, and K. Nurutdinov (2001), A new global mode of Earth deformation: Seasonal cycle detected, *Science*, **294**, 2342–2345.
- Blewitt, G., et al. (2005), A stable North American reference frame (SNARF): First release, paper presented at UNAVCO-IRIS Joint Workshop, UNAVCO Inc., Stevenson, Wash., 8–11 June.
- Davis, J. L., R. A. Bennett, and B. P. Wernicke (2003), Assessment of GPS velocity accuracy for the Basin and Range Geodetic Network (BARGEN), *Geophys. Res. Lett.*, **30**(7), 1411, doi:10.1029/2003GL016961.
- Ducea, M. (2001), The California Arc: Thick granitoid batholiths, eclogitic residues, lithospheric-scale thrusting and magmatic flare-ups, *GSA Today*, **11**, 4–10.
- England, P., and P. Molnar (1990), Surface uplift, uplift of rocks, and exhumation of rocks, *Geology*, **18**, 1173–1177.
- Erkan, K., and D. D. Blackwell (2008), A thermal test of the post-subduction tectonic evolution along the California transform margin, *Geophys. Res. Lett.*, **35**, L07309, doi:10.1029/2008GL033479.
- Freed, A. M., R. Bürgmann, and T. Herring (2007), Far-reaching transient motions after Mojave earthquakes require broad mantle flow beneath a strong crust, *Geophys. Res. Lett.*, **34**, L19302, doi:10.1029/2007GL030959.
- Gourmelen, N., and F. Amelung (2005), Postseismic mantle relaxation in the central Nevada seismic belt, *Science*, **310**, 1473–1476, doi:10.1126/science.1119798.
- Granger, D. E., and G. M. Stock (2004), Using cave deposits as geologic tiltmeters: Application to postglacial rebound of the Sierra Nevada, California, *Geophys. Res. Lett.*, **31**, L22501, doi:10.1029/2004GL021403.
- Hammond, W. C., C. Kreemer, and G. Blewitt (2008), Geodetic constraints on contemporary deformation in the northern Walker Lane: 3. Central Nevada seismic belt postseismic relaxation, in *Late Cenozoic Structure and Evolution of the Great Basin–Sierra Nevada Transition*, edited by J. Oldow and P. Cashman, Geol. Soc. of Am., Boulder, Colo., in press.

- Herring, T. A. (2002), GLOBK: Global Kalman filter VLBI and GPS analysis program, technical report, 98 pp., Dep. of Earth Atmos. and Planet. Sci., Mass. Inst. of Technol., Cambridge, Mass.
- House, M. A., B. P. Wernicke, and K. A. Farley (1998), Dating topography of the Sierra Nevada, California, using apatite (U-Th)/He ages, *Nature*, **396**, 66–69.
- Hudnut, K. W., Y. Bock, J. Galetzka, F. H. Webb, and W. H. Young (2001), The Southern California Integrated GPS Network (SCIGN), paper presented at 10th International Symposium on Crustal Deformation Measurement, Fed. Int. des Geometres, Orange, Calif., March 19–22.
- Jones, C. H., G. L. Farmer, and J. Unruh (2004), Tectonics of Pliocene removal of lithosphere of the Sierra Nevada, California, *Geol. Soc. Am. Bull.*, **116**, 1408–1422.
- King, R. W., and Y. Bock (2002), Documentation for the GAMIT GPS analysis software, technical report, 206 pp., Dep. of Earth Atmos. and Planet. Sci., Mass. Inst. of Technol., Cambridge, Mass.
- Langbein, J. (2008), Noise in GPS displacement measurements from southern California and southern Nevada, *J. Geophys. Res.*, **113**, B05405, doi:10.1029/2007JB005247.
- Le Pourhiet, L., M. Gurnis, and J. Saleeby (2006), Mantle instability beneath the Sierra Nevada mountains in California and Death Valley extension, *Earth Planet. Sci. Lett.*, **251**, 104–119.
- Malservisi, R., K. P. Furlong, and T. Dixon (2001), Influence of the earthquake cycle and lithospheric rheology on the dynamics of the eastern California shear zone, *Geophys. Res. Lett.*, **28**, 2731–2734.
- Mulch, A., S. A. Graham, and C. P. Chamberlain (2006), Hydrogen isotopes in Eocene river gravels and paleoelevation of the Sierra Nevada, *Science*, **313**, 87–89.
- Pelletier, J. D. (2004), Estimate of three-dimensional flexural-isostatic response to unloading: Rock uplift due to late Cenozoic glacial erosion in the western United States, *Geology*, **32**, 161–164.
- Saleeby, J., and Z. Foster (2004), Topographic response to mantle lithosphere removal in the southern Sierra Nevada region, California, *Geology*, **32**, 245–248.
- Saltus, R. W., and A. H. Lachenbruch (1991), Thermal evolution of the Sierra-Nevada: Tectonic implications of new heat-flow data, *Tectonics*, **10**, 325–344.
- Small, E. E., and R. S. Anderson (1995), Geomorphically driven late Cenozoic rock uplift in the Sierra-Nevada, California, *Science*, **270**, 277–280.
- Stein, R. S., and W. Thatcher (1981), Seismic and aseismic deformation associated with the 1952 Kern County, California, earthquake and relationship to the Quaternary history of the White Wolf Fault, *J. Geophys. Res.*, **86**, 4913–4928.
- Stock, G. M., R. S. Anderson, and R. C. Finkel (2005), Rates of erosion and topographic evolution of the Sierra Nevada, California, inferred from cosmogenic Al-26 and Be-10 concentrations, *Earth Surf. Processes Landforms*, **30**, 985–1006.
- Thatcher, W., and F. F. Pollitz (2008), Temporal evolution of continental lithospheric strength in actively deforming regions, *GSA Today*, **18**, 4–11, doi:10.1130/GSAT01804-5A.1.
- Wang, R., F. Lorenzo-Martin, and F. Roth (2006), PSGRN/PSCMP: A new code for calculating co- and post-seismic deformation, geoid and gravity changes based on the viscoelastic-gravitational dislocation theory, *Comput. Geosci.*, **32**, 527–541, doi:10.1016/j.cageo.2005.08.006.
- Wernicke, B., and G. J. Axen (1988), On the role of isostasy in the evolution of normal-fault systems, *Geology*, **16**, 848–851.
- Wernicke, B., and J. K. Snow (1998), Cenozoic tectonism in the central Basin and Range: Motion of the Sierran Great Valley block, *Int. Geol. Rev.*, **40**, 403–410.
- Wernicke, B., A. M. Friedrich, N. A. Niemi, R. A. Bennett, and J. L. Davis (2000), Dynamics of plate boundary fault systems from Basin and Range Geodetic Network (BARGEN) and Geologic Data, *GSA Today*, **10**, 1–7.
- Zandt, G., H. Gilbert, T. J. Owens, M. Ducea, J. Saleeby, and C. H. Jones (2004), Active foundering of a continental arc root beneath the southern Sierra Nevada in California, *Nature*, **431**, 41–46.

R. A. Bennett, N. P. Fay, and S. Hreinsdóttir, Department of Geosciences, University of Arizona, Tucson, AZ 85721, USA. (nfay@email.arizona.edu)